Author: D. M. Deery, J. B. Passioura, J. R. Condon and A. Katupitiya

Title: Uptake of water from a Kandosol subsoil. II. Control of water uptake by roots

Journal: Plant and Soil **ISSN**: 0032-079X 1573-5036

Year: 2013 **Volume:** 368 **Issue:** 1-2 **Pages:** 649-667

Abstract: Aim: To test for the presence of an impediment to water flow at the soil-root interface. Methods: Wheat plants were grown in repacked and undisturbed field soil. Their transpiration rate, E, was varied in several steps from low to high and then back to low again, while the hydrostatic pressure in the leaf xylem, ψ_{xylem}, was measured non-destructively and continuously. These measurements were compared to a mathematical model that calculated ψ_{xylem} by assuming that the hydraulic resistance across the plant was constant and that the radial flow of water to unit length of a typical plant root generated gradients in pressure in the soil water. Results: For the repacked soil, the radial flow model could not match the experiment during the falling phase of E, unless it was assumed that either an additional, constant, interfacial resistance between the soil and the roots had developed when E was large and ψ_{xylem} was rapidly falling, or that the resistance within the plant had changed. For the undisturbed field soil, the radial flow model did not agree with the experiment. Plausible agreement was achieved when plant water uptake was accounted for using a distributed sink model in HYDRUS-1D, with E integrated across the rootzone. This approach was based on the measured large variation in the vertical distribution of roots. Conclusions: There was no strong evidence of large drawdowns of soil water in the rhizosphere, even when ψ_{xylem} was falling rapidly when E was large and the soil was moderately dry. Thus, there seems to have been an additional impediment to water flow from soil to plant, either within the plant, or at the interface between the two.

DOI/URL: http://dx.doi.org/10.1007/s11104-013-1736-7 http://researchoutput.csu.edu.au/R/-?func=dbin-jump-full&object_id=46361&local_base=GEN01-CSU01

Author Address: david.deery@csiro.au **CRO Number:** 46361

Title

Uptake of water from a Kandosol subsoil. II. Control of water uptake by roots

Authors

David M. Deery*
Ph: 61 2 6246 4869
Fax: 61 2 6246 4975
david.deery@csiro.au
High Resolution Plant Phenomics Centre, CSIRO Plant Industry
Clunies Ross St Black Mountain,
Canberra ACT 2601

John B. Passioura
CSIRO Plant Industry
Clunies Ross St Black Mountain,
Canberra ACT 2601

Jason R. Condon
EH Graham Centre, Charles Sturt University, School of Agricultural and Wine Sciences
Wagga Wagga NSW 2678 Australia

Asitha Katupitiya
Charles Sturt University, School of Agricultural and Wine Sciences
Wagga Wagga NSW 2678 Australia

Keywords

Radial flow model; HYDRUS-1D; root water uptake; subsoil; rhizosphere

Title

Uptake of water from a Kandosol subsoil. II. Control of water uptake by roots

Abstract

Aims

Annual crops typically fail to extract substantial amounts of seemingly available water from the bottom third of their rooting zones by maturity. Mechanistic understanding of what limits the uptake of residual water remains poor.

Methods

Wheat plants were grown in repacked and undisturbed field soil where the transpiration rate, E, and the hydrostatic pressure in the leaf xylem, ψ_{xylem}, were measured non-destructively and continuously. These measurements were compared to a model that calculates ψ_{xylem} by simulating the radial flow of water to unit length of typical plant root.

Results

For the repacked soil, the radial flow model could not match the experiment during the falling phase of E, unless it was assumed that an additional, constant, interfacial resistance between the soil and the root had developed when E was high and ψ_{xylem} was rapidly falling. For the undisturbed soil, the radial flow model did not agree with the experiment. The distributed sink utilised by HYDRUS-1D was in much closer agreement.

Conclusions

The constant interfacial resistance may have been caused by the roots shrinking when E was high and ψ_{xylem} was rapidly falling. Limitations to water uptake may reside more within the roots than the soil.

Abbreviations

Introduction

The extraction of water from the subsoil by wheat crops during grain-filling is especially valuable to grain yield (Kirkegaard et al. 2007; Angus and Herwaarden 2001). Kirkegaard et al. (2007) found that subsoil water used after flowering increased grain yield by 0.6 t ha^{-1}, an efficiency of 59 kg of grain per ha per mm of water used. This is nearly three times the well-established benchmark of wheat grain produced per mm of water used throughout the growing season in south eastern Australia, namely 20-22 kg ha^{-1} mm^{-1} (French and Schultz 1984; Sadras and Angus 2006). However Kirkegaard et al. (2007) found that despite the appreciable efficiency of subsoil water use, the crop failed to extract all of the water seemingly available to it.

Several hypotheses have been proposed as to why the extraction is incomplete. These include: that the flow rate of water through soil to individual, though well-distributed, roots is limited by the hydraulic properties of the soil (Philip 1957; Gardner 1960; Cowan 1965); that there is a large interfacial resistance to the flow of water between soil and root (Bristow et al. 1984), possibly exacerbated by root shrinkage and vapour gaps (Herkelrath et al. 1977a; Carminati et al. 2009); that the roots are clumped in biopores, so that water must move long distances to them (Passioura 1991); and that there may be a large osmotic pressure close to the root surface if solutes, excluded by the root as the water enters, increase in concentration at the root surface (Stirzaker and Passioura 1996).

This paper investigates these hypotheses by comparing; (a) simultaneous experimental measurements of the plant transpiration rate, E [μg s^{-1}], and the hydrostatic pressure in the leaf xylem, ψ_{xylem} [kPa], with (b) the output of a mathematical model that calculates ψ_{xylem}. Experimentally, ψ_{xylem} is taken to be equal and opposite to the pressure, herein termed balancing pressure, P [kPa], required to bring the pressure in the leaf xylem to atmospheric pressure when the pot in which the roots are growing is enclosed within a pressurised chamber (Passioura and Munns 1984).

The model solves the radial diffusion equation for the flow of water to a unit length of plant root, assumed to be typical of all roots. It calculates the putative pressure drop, $\Delta\psi_{soil}$, between the water in the bulk soil, ψ_{bulk}, and that at the root surface. The model assumes that the hydraulic resistance within the plant in any given experiment, R_{plant}, pertains when E is large and non-linearities in $P(E)$ appear. Previous studies using the same experimental system have shown R_{plant} to be demonstrably constant when E is small (Passioura 1980; Stirzaker and Passioura 1996). R_{plant} is taken to be the slope of P with respect to E, i.e. $-d(\psi_{xylem})/dE$ when E is small. The pressure drop across the plant, $\Delta\psi_{plant}$, is then defined as the product of E and R_{plant}.

Eq. 1 summarises the terms that comprise ψ_{xylem}, including a term to account for possible interfacial and osmotic effects at the root soil interface ($\Delta\psi_{R\text{-}S}$):

$$\psi_{xylem} = \Delta\psi_{plant} + \Delta\psi_{soil} + \psi_{bulk} + \Delta\psi_{R-S} \quad (1)$$

Fig. 1 shows these, plus the main inputs and the experimental measurements, schematically. Note that $\Delta\psi_{R\text{-}S}$ is not explicitly modelled or experimentally measured in this system. However, it follows that if all the other terms in Eq. 1 are accounted

for, then $\Delta\psi_{R\text{-}S}$ can be evaluated if there is a difference between the experiment and model.

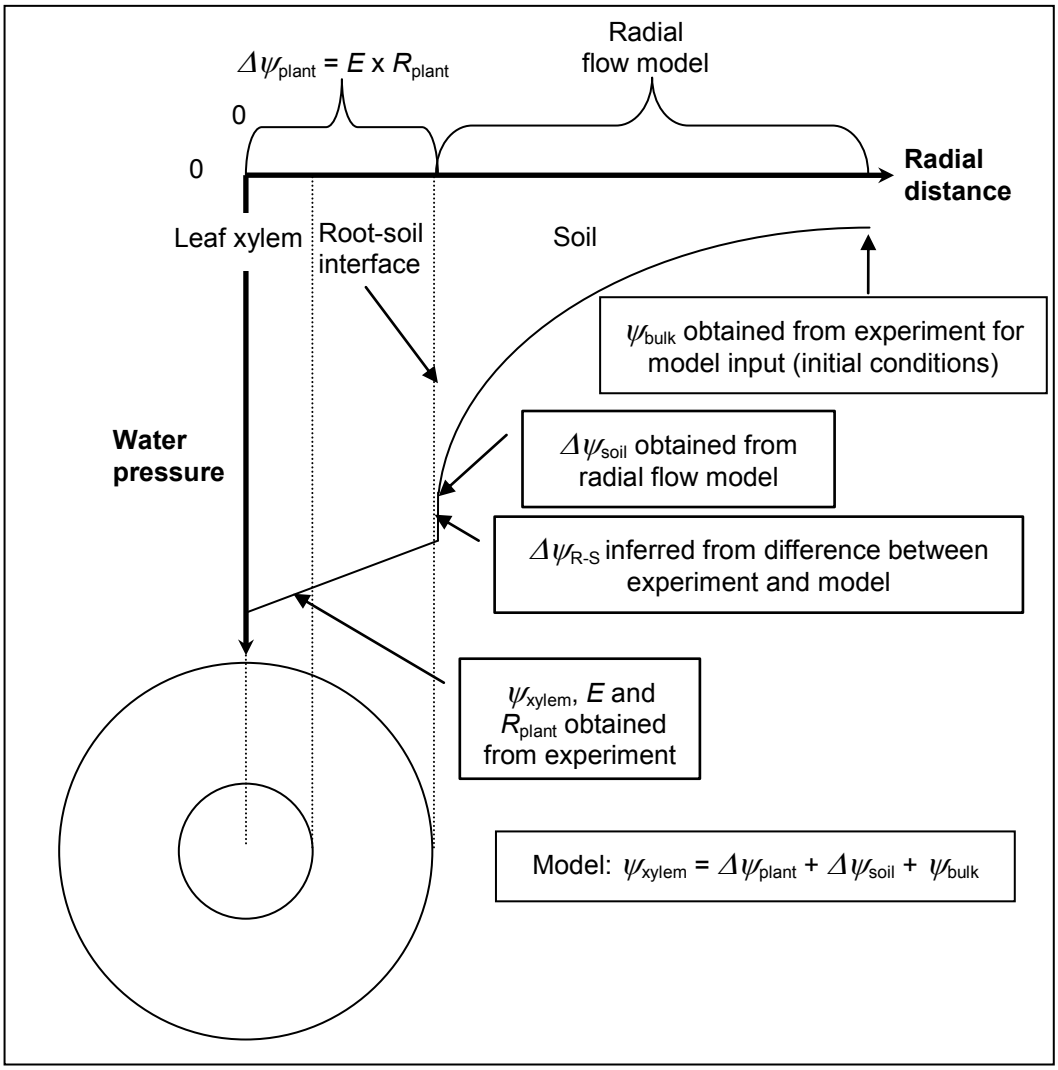

Fig. 1 Schematic of the system to be modelled. Axis showing radial distance away from the xylem centre is shown at the top from left to right. Axis for increasingly negative water pressure is shown on the left. Note that $\Delta\psi_{R\text{-}S}$ is not explicitly modelled or measured, but evaluated from difference between experiment and model. Note that ψ_{xylem} refers to the leaf xylem.

This paper investigates both undisturbed and repacked soil. The undisturbed field soil is likely to be heterogeneous in both soil hydraulic properties and root distribution, including the possible clumping of roots in channels made by previous roots (White and Kirkegaard 2010). The repacked soil is a simpler system, in which assumptions of homogeneous soil hydraulic properties and uniform root distribution are more likely to be met. It therefore offers a contrast for helping to interpret the behaviour in the undisturbed soil, which is the environment experienced by crop plants growing in the field.

Materials and methods

Experimental

Soil types

Three soil types were used: undisturbed clay-loam, repacked clay-loam and repacked sand. These soil types are representative of two major wheat growing areas in Australia; the sand is from the wheat belt in Western Australia (31^o 50' S, 118^o 22' E) and the undisturbed and repacked clay-loam is from the New South Wales southwest slopes in south-eastern Australia (34^o 43' S, 147^o 48' E) and is classified red Kandosol (Isbell 2002). This is the same site as that used in the study of Kirkegaard et al. (2007). They found that a single calibration curve for the neutron moisture meter could be used for all depths at 0.2 m and below. The error for estimation of volumetric water content was 0.013 [m^3 m^{-3}], thereby discounting depth dependant properties within the soil profile for the purpose of this study. The soil profile down to 2 m depth is described in greater detail by Kirkegaard et al. (2007) (refer their Table 1).

The undisturbed soil was sampled by firstly exposing an undisturbed horizontal shelf of soil at 20 cm below the soil surface (B horizon) and then using a hydraulic press to force a stainless steel cylinder, 20 cm in length by 8.6 cm ID, vertically into the soil. The stainless steel cylinder, containing the undisturbed soil sample, was then extracted by removing the soil from around the cylinder. The bulk density of the undisturbed clay-loam soil was 1.6 g cm^{-3}.

The repacked clay-loam was collected from a depth of 20 to 40 cm, sieved to less than 2 mm and repacked to a bulk density of 1.3 g cm^{-3}, substantially lower than that in the undisturbed soil because roots would not grow in this soil repacked to the original 1.6 g cm^{-3}. The sand was collected from a depth of 20 to 40 cm, sieved to less than 2 mm and repacked to a bulk density of 1.6 g cm^{-3}.

Soil water retention

For all three soil treatments, the soil water retention was measured using a standard tension table at 10 kPa suction and pressure plate apparatus at 100, 500, 1000 and 1500 kPa suction. Soil water retention measurements were made on six replicate soil cores for the undisturbed clay-loam and three each for both the repacked clay-loam and repacked sand. The dimensions of the soil cores were 3.6 cm in length by 4.8 cm inside diameter.

For each suction and soil treatment, the mean soil water retention was calculated from the above mentioned replicates and the van Genuchten (1980) function (eq. 2) was then fitted using the minimum sum of squares criterion to optimize the four independent parameters.

$$\theta(\psi_{soil}) = \theta_r + \frac{\theta_s - \theta_r}{\left[1 + \left|\alpha\psi_{soil}\right|^n\right]^{(1-1/n)}} \qquad (2)$$

Where θ_r and θ_s denote the residual and saturated soil water content respectively, α and n are shape parameters and ψ_{soil} is the soil water potential. The means of the measured soil water retention and the fitted van Genuchten (1980) retention function (eq. 2) for all three soil types are shown in Fig. 2.

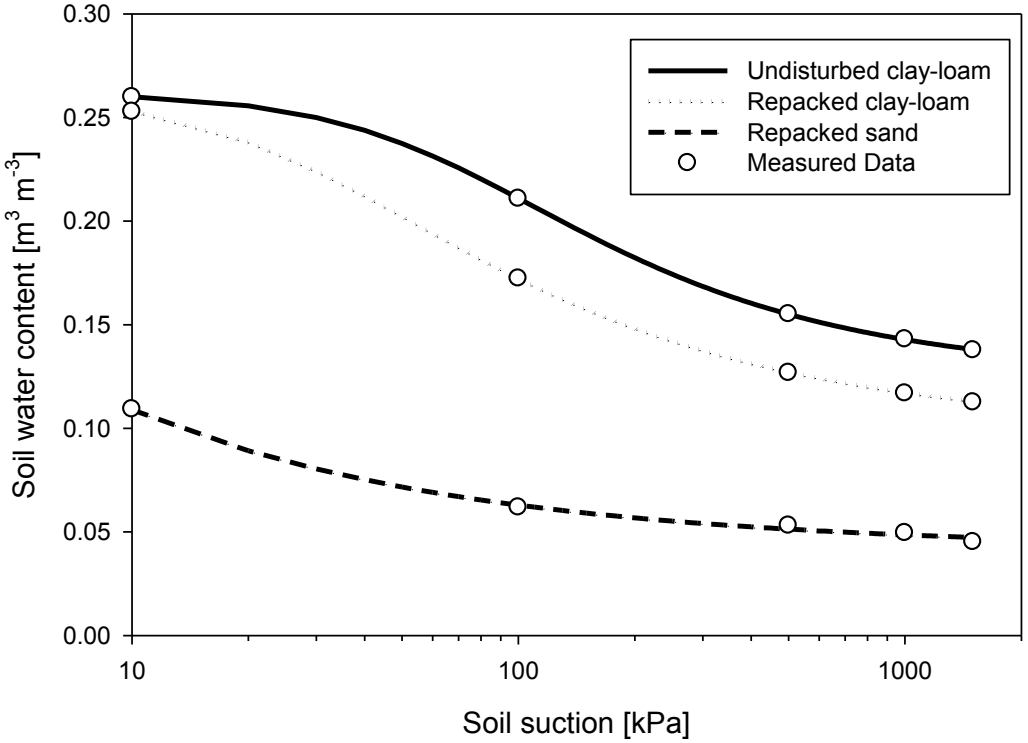

Fig. 2 Measured soil water retention (circles = mean of n replicates) and fitted (lines) van Genuchten (1980) retention function (eq. 2) for undisturbed clay-loam (n = 6), repacked clay-loam (n = 3) and repacked sand (n = 3).

Soil water diffusivity

The soil water diffusivity, $D(\theta)$, for each soil type was measured using the method described in part I of this series (Deery et al. 2012) . Briefly, undisturbed and repacked soil cores were initially equilibrated at a soil water suction of 10 kPa. The base of each core was sealed, and the top exposed to a turbulent atmosphere after the core was placed on a recording balance. The cumulative evaporation with time was thereby recorded. $D(\theta)$ was then determined by solving the one dimensional flow equation numerically, with $D(\theta)$ assumed to be either quadratic or exponential in form, with parameters that were adjusted at each iteration until the calculated cumulative evaporation converged to close to the actual. As in part I of this series (Deery et al. 2012), $D(\theta)$ was also calculated using the analyses of Doering (1965) and Passioura (1977).

$D(\theta)$ was determined from the following number of sample replicates collected from the same locations described previously; undisturbed clay-loam, three replicate soil cores, ran twice each (n = 6); repacked clay-loam, three replicate soil cores, ran once each (n = 3) and repacked sand; three replicate cores, ran once each (n = 3). The mean D of the n replicates for a given analysis was then calculated throughout the measurement range of θ and is presented in Fig. 3 with the soil suction from 100 to 1500 kPa.

For the undisturbed clay-loam, the $D(\theta)$ analyses of Deery et al. (2012), Doering (1965) and Passioura (1977) all converged to ~10×10^{-9} m^2 s^{-1} (Fig. 3). Fig. 3 shows

that $D(\theta)$ is close to constant when the soil suction is drier than 500 kPa. However, the agreement between the analyses of Deery et al. (2012), Doering (1965) and Passioura (1977) is not as good for the repacked clay-loam and the repacked-sand. For the repacked clay-loam, the exponential $D(\theta)$ and analysis of Doering (1965) agree with each other, while the analysis of Passioura (1977) and quadratic $D(\theta)$ are about 25% above and below respectively. For the repacked-sand, all the analyses except the quadratic are in accord with each other. Given the variability of $D(\theta)$ among the four analyses for the repacked clay-loam and the repacked-sand, and the near constant D when the soil suction was drier than ~500 kPa for the repacked clay-loam and ~100 kPa for the repacked sand, a constant D proximal to the lower limit of that measured was chosen for modelling the flow of water to the plant roots for the repacked clay-loam and repacked sand. This equated to $10x10^{-9}$ m^2 s^{-1} for the repacked clay-loam and $1x10^{-9}$ m^2 s^{-1} for the repacked sand.

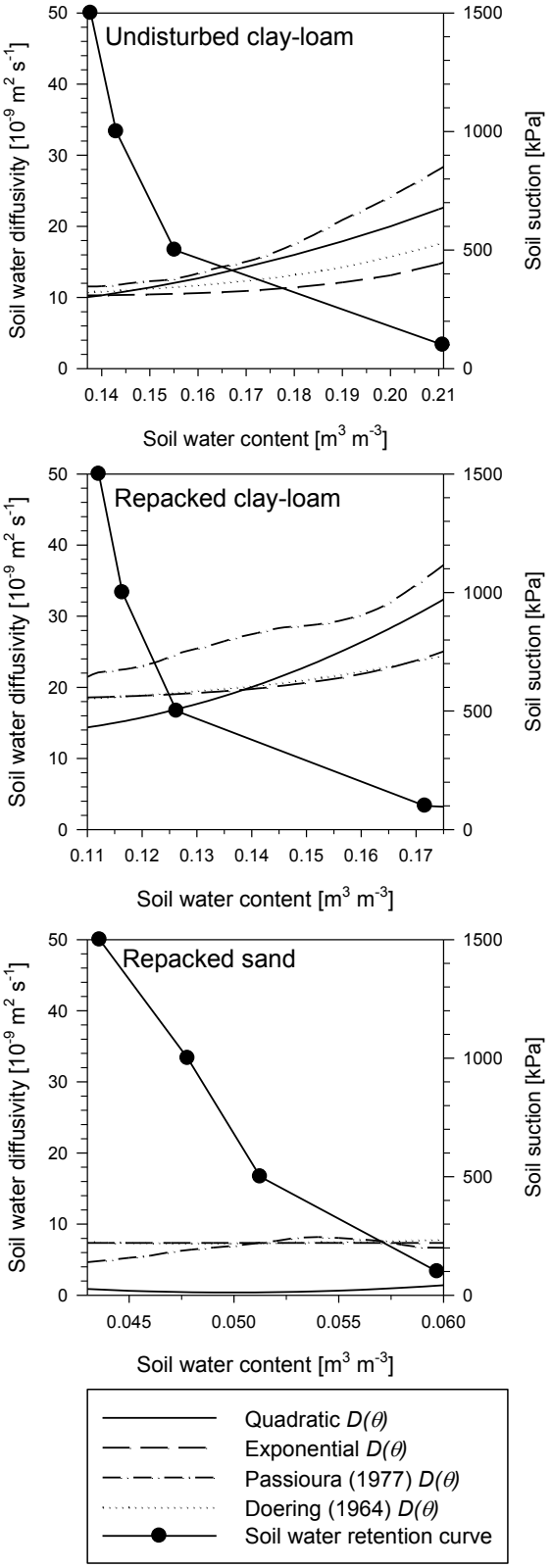

Fig. 3 $D(\theta)$ for each soil type plotted with soil suction. $D(\theta)$ measurements were made using the method described in part I of this series (Deery et al. 2012) and are presented as the mean of n replicates. Undisturbed clay-loam: three replicate cores, ran twice each (n = 6). Repacked clay-loam: three replicate cores, ran once each (n = 3). Repacked sand: three replicate cores, ran once each (n = 3).

Preparation of the soil

The repacked soil was contained in pots made of PVC that were 20 cm long by 8.6 cm inside diameter (ID), with a volume of 1160 cm^3. The soil was packed in 1 cm increments using an arbor press with a cylindrical piston just smaller than the ID of the pot, thereby ensuring that the bulk density was uniform with depth.

All of the repacked pots were leached with 1000 cm^3 (about twice the pore volume) of half strength Hoagland's solution (Hoagland and Arnon 1950) (26 kPa osmotic pressure). Each core was equilibrated at a suction of 10 kPa at the base of the pot. The base of each core was then covered with plastic Petri dishes containing four 2 mm diameter holes to allow gas exchange.

The undisturbed core was supplied with 4 mL each of Hoagland's (Hoagland and Arnon 1950) A and B stock solution augmented with phosphorus in the form of 3 mL of 0.5 Molar $K_2H_2PO_4$ (75 mg P). Each of the three solutions were applied to a different location on the top of the core at three equidistant points on the pot circumference. The solutions were applied as discrete sources on the top edges of the core, thereby allowing the roots to access nutrients within them without disturbing the low nutrient status of the bulk of the soil, from which almost all water uptake would occur.

Preparation of the plants

A metal cap was fitted to the top of each core (Passioura and Munns 1984; Stirzaker and Passioura 1996). A small hole located in the centre of the metal cap allowed the cores to be sown with a germinated wheat seed (*Triticum aestivum* cv. Janz). The hole in the cap around the stem was filled with silicone rubber after the plants were well established, to form a gas-tight seal. The plant and pot were then moved to a growth chamber maintained at a day/night temperature of 11^oC with a daily photoperiod of 10 h and photon flux density of 350 $\mu m\ m^{-2}\ s^{-1}$ maintained at the leaf level.

Total leaf area was estimated as the sum of the length [cm] x breadth [cm] x 0.78 for each leaf, measured by ruler (Termaat et al. 1985). The multiplier of 0.78 is used to account for the ellipse shape of the leaf. Once the leaf area of the plants had reached about 20 cm^2, which usually took around 20 days after sowing, measurements of *P* and *E* were made every second or third day depending on how fast the plant was depleting the soil water. The leaf area was measured prior to the start of each set of measurements.

Experimental apparatus

Simultaneous measurements of *E* and *P* were made using essentially the experimental method described in Passioura and Munns (1984) and Stirzaker and Passioura (1996). The experimental setup is shown schematically in Fig. 4. The method is described in more detail in Deery (2008). A pot was put in a pressure chamber and the shoot of the plant, which remained outside the pressure chamber, was enclosed inside a cuvette. The evaporative demand on the plant was varied by varying the light intensity and the humidity, and *E* was measured as the product of the flow rate of air passing through the cuvette and the difference in humidity between the ingoing and outgoing air. *P* was measured by applying just enough pressure in the root chamber to bring a cut in a leaf to the point of bleeding.

The leaves inside the cuvette were illuminated horizontally by a 400 W metal halide lamp that provided a photosynthetic photon flux density ranging between 70 and 500 μmol m^{-2} s^{-1}. The photon flux density was adjusted by removing and replacing wire mesh screens (0.5 mm wire thickness, 1 mm^2 aperture) from in front of the lamp. With both screens in front of the light source the photon flux density was approximately 75 μmol m^{-2} s^{-1} and 240 and 500 μmol m^{-2} s^{-1} when the first and second screens were removed, respectively.

The temperature of the pressure chamber that contained the soil core and plant roots was controlled at a constant temperature of 11°C; this is a similar temperature to that experienced by the roots growing in the subsoil in the field during the growing season.

Air was passed through the cuvette at flow rates ranging from 1.8 to 12 L min^{-1}. The humidity of the ingoing and outgoing air from the cuvette was measured in either one of two ways; (1) simultaneously with two dew-point hygrometers (General Eastern model Dew-10-xx1, accuracy +/–0.5°C, repeatability +/–0.05°C) or (2) with one dewpoint hygrometer, where the ingoing and outgoing air-streams were switched through the dewpoint hygrometer every 5 min. The transpiration rate was calculated as the product of the flow rate through the cuvette and the difference in humidity between the ingoing and outgoing air.

The stomatal conductance, g [mol m^{-2} s^{-1}], was estimated using eq. 3 where p_{atm} is the atmospheric pressure (assumed to be 1013 hPa), F_{air} [m^3 s^{-1}] is the flow rate of air through the cuvette, V_m [m^3 mol^{-1}] is the molar volume of an ideal gas at the given temperature, LA [m^2] is the leaf area and VPD [hPa] is the estimated vapour pressure deficit between the stomatal cavity inside the leaf and ambient air inside the cuvette. The vapour pressure inside the stomatal cavity of the leaf is estimated using the measurement of leaf temperature, where saturated conditions inside the stomatal cavity are assumed.

$$g = \frac{p_{atm}}{VPD} * \frac{F_{air}}{V_m} * \frac{1}{LA} \tag{3}$$

The conditions inside the cuvette were varied to increase the evaporative demand in a series of steps (Table 1). At each step the air flow, humidity and light intensity settings were maintained until the control system was steady and a reliable measurement of E could be made; this usually took 30 min. However when it became clear that P was starting to increase non-linearly with E, and the relationship between P and E was no longer stable with time, the current evaporative demand setting was maintained until P began approaching the limit of the equipment, 2000 kPa. At which point the evaporative demand was decreased and the sequence of steps reversed to investigate the falling E phase (discussed further in "Calculation of $\Delta\psi_{plant}$ and ψ_{bulk}").

Table 1 Evaporative demand settings imposed on the plant inside the cuvette. Each setting is usually applied for 30 min to enable steady state conditions. When the greatest evaporative demand is obtained the sequence is reversed to investigate any hysteresis.

Setting No.	Air flow [L min^{-1}]	Vapour density [g m^{-3}]	Light intensity [μmol m^{-2} s^{-1}]
1	1.8 to 2.0	12.0 to 15.0	75
2	2.4 to 2.6	6.5 to 7.0	75
3	3.0 to 3.0	6.5 to 7.0	240
4	3.5 to 3.6	4.5 to 5.5	240
5	4.0 to 4.5	4.5 to 5.5	500

The pressure inside the root chamber was adjusted automatically by a control system that kept the exposed xylem on a cut leaf on the point of bleeding. An infrared sensor determined the position of the meniscus in a capillary tube that was connected hydraulically with the exposed xylem, and the controller responded to the signal from the sensor by adjusting the pressure to keep the position of the meniscus at a set point – i.e. if the meniscus rose, the controller lowered the pressure to bring the meniscus back to the set point, and vice versa. Hydraulic continuity was maintained by using a nylon (hydrophilic) tube that remained filled with water despite a small suction generated by the meniscus being a few mm below the exposed xylem. The suction is necessary to induce a flow into the tube if the xylem is exuding. The nylon tube is kept in hydraulic continuity with the xylem by means of a patch of filter paper which provides a water-saturated bridge between the xylem and the closely adjacent tube. The connection was wrapped in a small piece of plastic film to protect it against evaporative loss.

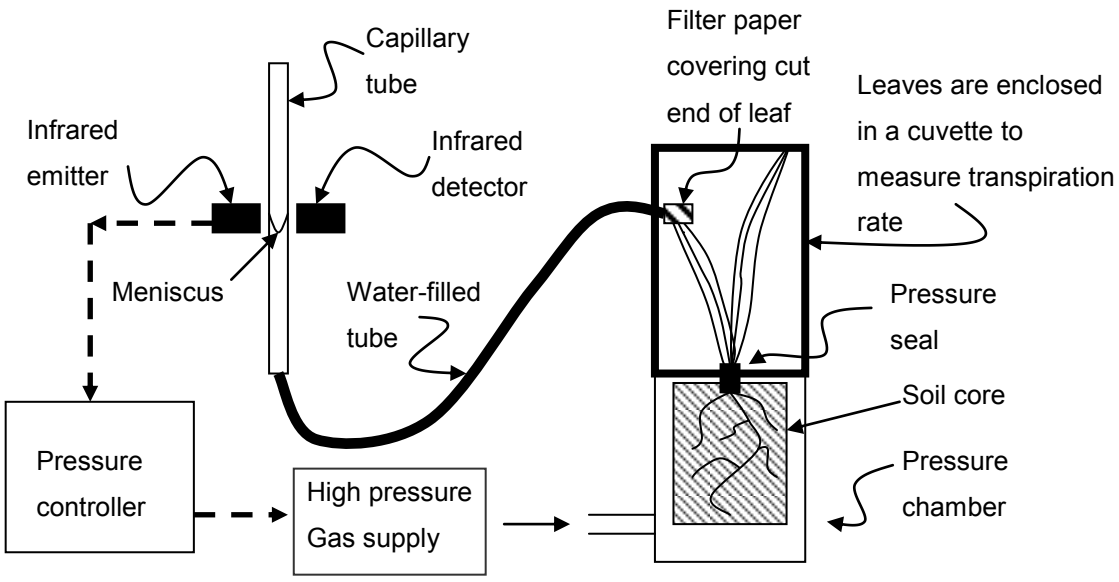

Fig. 4 Schematic of equipment used to measure pressure drop across the plant and soil. The infrared emitter and detector form a position sensor that monitors the position of the meniscus inside the capillary tube. The position sensor is connected to a pressure controller that regulates the pressure inside the pressure chamber. Drawing not to scale.

Determination of root length and diameter

The length and diameter of the roots were determined for each soil type after the experiment using the same method as Watt et al. (2005). The roots were washed from the soil and scanned on an Epson 1680 modified flatbed scanner and the images analysed using WINRhizo software (Régent Instruments Inc. Québec, CA). The roots were preserved in 50% ethanol and prior to scanning, rinsed in water then stained in 0.05% toluidine blue (pH 4.4) for 3 min, rinsed again in water and then transferred to a clear Perspex tray containing a shallow film of water for scanning. For the undisturbed core roots, the wheat roots were separated from the roots remnant from previous crops prior to scanning, as described in Watt et al. (2008).

Calculation of $\Delta\psi_{plant}$ and ψ_{bulk}

Fig. 5 shows an example of the relation between P and E for a wheat plant growing in wet soil across a low to high range of E. Note that the cross-sectional area of the pot is 58 cm^2, thereby equating E of 400 $\mu g\ s^{-1}$ to 6.0 mm day^{-1}. When P is a linear function of E (Fig. 5), as it typically is at low E, the data can be interpreted with a simple linear function:

$$P = R_{plant} \times E + \psi_{bulk} \quad (4)$$

Where R_{plant} [kPa s μg^{-1}] is the hydraulic resistance of the plant and ψ_{bulk} [kPa] is the water suction in the bulk soil. When the soil water is at equilibrium, the pressure drop across the air water interface of all the water filled pores in the bulk soil is ψ_{bulk}; which is shown as the intercept on the axis in Fig. 5 as ψ_{bulk} at the start of the experiment (Stirzaker and Passioura 1996; Passioura and Munns 1984; Passioura 1980) .

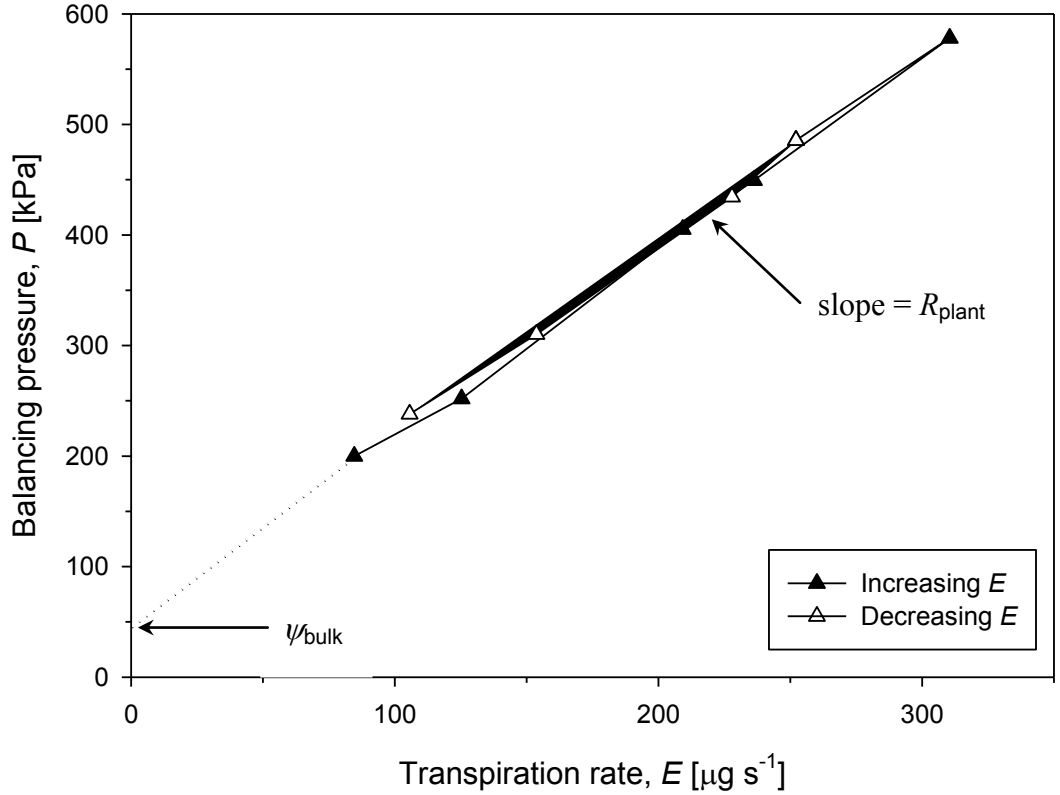

Fig. 5 Balancing pressure, P, of a wheat plant plotted as a function of increasing and decreasing transpiration rate, E, showing ψ_{bulk} and R_{plant} (eq. 4).

However, the intercepts of the rising and falling E phases only provide valid estimates of ψ_{bulk} if the difference between ψ_{soil} at the root surface and in the bulk soil, $\Delta\psi_{soil}$, is negligible. A good indicator of which is that the slope of $P(E)$ is constant and independent of E (e.g. Fig. 5) – for if $\Delta\psi_{soil}$ is not negligible, it will increase rapidly with E as the water content, and thence the exponentially related water pressure, falls at the root surface. This proviso extends further to the estimate of R_{plant}; which is only valid if $\Delta\psi_{soil}$- is negligible.

The intercepts of the rising and falling E phases (ψ_{bulk}) were compared to ψ_{soil} determined from the average θ by weighing the pot before and after the experiment. The intercepts (ψ_{bulk}) and the average soil water content determined by weight, provide estimates of the averaged ψ_{soil} over the entire rhizosphere at the start and finish of the experiment. The analytical analysis of van Lier et al. (2006) found that the mean soil water content occurred at a distance 0.6065 times the half distance between the roots. However, their numerical analysis showed that this distance varies with soil type, root length density and transpiration rate. They concluded that for most simulations, the value was around 0.53.

The analytical analysis of van Lier et al. (2006) found that the mean soil water content occurred at a distance 0.6065 times the half distance between the roots. However, their numerical analysis showed that this distance varies with soil type, root length density and transpiration rate. They concluded that for most simulations, the value was around 0.53.

Plant water uptake model

Radial flow model

The plant water uptake was modelled using the radial diffusion equation, eq. 5, subject to the initial and boundary conditions in eq. 6. The radial diffusion equation calculates the flow of water to a unit length of plant root, assumed to be typical of all roots.

$$\frac{\partial\theta}{\partial t} = \frac{1}{r}\frac{\partial}{\partial r}\left(rD\frac{\partial\theta}{\partial r}\right) \tag{5}$$

$$\begin{aligned} &t = 0, \quad r_a \le r \le r_b, \quad && \theta = \theta_i \\ &t > 0, \quad r = r_a, \quad && D(\theta)\frac{\partial\theta}{\partial r} = \frac{Q\left(r_b^2 - r_a^2\right)}{2r_a} \\ &t > 0, \quad r = r_b, \quad && \frac{\partial\theta}{\partial r} = 0 \end{aligned} \tag{6}$$

Where r [m] is radial distance from the root, θ_i is the initial soil water content determined experimentally from ψ_{bulk} and Fig. 2, Q [m^3 m^{-3} s^{-1}] is the rate of extraction of water from the soil, r_a is the root radius and r_b is an estimate of half the average distance between adjacent roots, derived from the root length density (length of root per volume of soil), L_v, as follows:

$$r_b = 1/\sqrt{\pi L_v} \tag{7}$$

The experimental data, including the transpiration rate, E (converted from [μg s^{-1}] to [m^3 s^{-1}]), and the volume of the pot, *svol* [m^3], was used to define the variable flux boundary condition at r_a (eq. 6):

$$Q = \frac{E}{svol} \tag{8}$$

Eq. 5 was solved numerically, using the finite difference method and Jacobian analysis described in Campbell (1985) , by setting:

$$R = \ln(r/r_a) \tag{9}$$

The log transform reduces the number of distance steps needed in the finite difference grid, especially if (r/r_a) is large (Passioura and Cowan 1968). Substituting eq. 9 into eq. 5 gives,

$$\frac{\partial \theta}{\partial t} = \frac{e^{-2R}}{r_a^2}\frac{\partial}{\partial R}\left(D\frac{\partial \theta}{\partial R}\right) \tag{10}$$

with:

$$\begin{aligned} &t = 0, \quad 0 \le \ln(r_b/r_a) \le R_b, && \theta = \theta_i \\ &t > 0, \quad R = 0, && D(\theta)\frac{\partial \theta}{\partial R} = \frac{1}{2}Q\left(r_b^2 - r_a^2\right) \\ &t > 0, \quad R = R_b, && \frac{\partial \theta}{\partial R} = 0 \end{aligned} \tag{11}$$

The model was run for each experiment with a range of values of effective root length density and the optimal fit was determined by trial and error. This is because it is unlikely that that whole of the measured root length density would be taking up water, an issue that has been studied by many (Bristow et al. 1984; Herkelrath et al. 1977b; Lang and Gardner 1970; Stirzaker and Passioura 1996). Further, in the case of the undisturbed soil, likely clumping of the roots in pre-existing channels (White and Kirkegaard 2010) may reduce the effective root length density to as low as the length of occupied channel per unit volume of soil (Passioura 1991).

Model description for the undisturbed clay-loam soil

For the undisturbed clay-loam soil, given the large difference between ψ_{soil} determined from the average θ in the pot before the experiment and the intercept on Fig. 6(a), shown in Table 3, and that the roots were concentrated at the top of the pot (Table 2), it seems likely that the extraction of water by the roots was constrained to some unknown soil volume at the top the pot. The height of this unknown section of the pot was estimated by assuming:

(1) That the large intercept of 760 kPa (Table 3) at the start of the experiment implied an average θ of 0.147 (from Fig. 2) in the upper portion of the pot to which the extraction of water by the roots was supposedly confined, and
(2) that the uptake of soil water by the roots from the time the pot had been rewatered to the start of the experiment on which Fig. 6(a) is based, had gone only from the zone where extraction of water by the roots was supposedly confined.

The measured uptake of water was 36 g, and the pot had been rewatered to an average θ of 0.241. Thus the volume from which the water had been lost was about 380 cm^3 (volumetric loss of water (36 cm^3) divided by the change in θ of 0.094), which was about one third of the pot's volume (1160 cm^3).

The experiment was then modelled with the roots confined to the top third of the total soil volume (Fig. 6(a)), a constant D of 10×10^{-9} m^2 s^{-1} (as measured, Fig. 3) and L_v of 28.7 cm cm^{-3} (Table 2). It is clear from Fig. 6 that confining the roots to the top third resulted in a large overestimation of P. Subsequently, the experiment was modelled several times by varying the following parameters in the model; (a) root length density, L_v, (10.0 to 0.5 cm cm^{-3}), (b) diffusivity, D (10×10^{-9} to 1×10^{-9} m^2 s^{-1}) and (c) the volume of soil occupied by the roots (top 33 to 90% of the pot volume). None of these changes resulted in a good fit between the experiment and the radial flow model.

Alternatively, water may have moved from lower in the pot towards the top third, where the roots were concentrated. We investigated this possibility by using the HYDRUS-1D (one-dimensional) numerical soil water flow model (Simunek et al. 2008). The HYDRUS-1D program numerically solves the Richards flow equation for variably saturated water flow and incorporates a distributed sink term to account for water uptake by plant roots (eq. 12).

$$\frac{\partial \theta}{\partial t} = \frac{\partial}{\partial x}\left(K \frac{\partial h}{\partial x} \right) - S(h) \tag{12}$$

Where h [m] is the water pressure head, K [m s^{-1}] is the unsaturated hydraulic conductivity and S [m^3 m^{-3} t^{-1}] is the distributed sink term to account for water uptake by plant roots. The distributed sink term, S, (eq. 13) incorporates the potential root water uptake rate, S_P, and a dimensionless stress response function, α. This stress response function was set to unity in the analysis, so that the modelled E from HYDRUS-1D matched the actual E from the experiment. E from the experiment was scaled to one-dimensional units for the HYDRUS-1D simulation by dividing by the cross-sectional area of the pot.

$$S(h) = \alpha(h) S_P \tag{13}$$

In the HYDRUS-1D simulation, S_P was equally distributed over the root zone according to eq. 14, where L_R is the depth of the root zone, set equal to the top one third of the pot, and T_P is the potential transpiration rate, set to E from the experiment (Fig. 6).

$$S_P = \frac{1}{L_R} T_P \tag{14}$$

In summary, the input data for the HYDRUS-1D simulation was as follows; soil hydraulic properties (Fig. 2 and Fig. 3), length of pot (0.2 m), initial soil suction for top third (760 kPa) and bottom two thirds (102 kPa) (Table 3), E and time from experiment (Fig. 6), homogenous root distribution and uniform potential extraction for the top third of the pot.

The results were plotted (Fig. 6) using eq. 4 to estimate the balancing pressure, P, where ψ_{bulk} was assumed to equal the mean suction in the rootzone (top third) from the HYDRUS-1D simulation. From this simulation, it seems that the movement of water from the lower layer in the pot to the top one during the experiment may have kept P within the bounds shown in Fig. 6.

Results

The measurements of root diameter, total root length and root length density for the undisturbed clay-loam (UCL), repacked clay-loam (RCL) and repacked sand (RS) are shown in Table 2.

Table 2 Measurements of root diameter, total root length and root length density for undisturbed clay-loam (UCL), repacked clay-loam (RCL) and repacked sand (RS).

Depth [cm]	Average root diameter [mm]			Total root length [m]			Root length density [cm cm^{-3}]		
	UCL	RCL	RS	UCL	RCL	RS	UCL	RCL	RS
0-5	0.26	0.27	0.27	83.5	30.8	8.0	28.7	10.8	2.9
5-10	0.31	0.30	0.27	4.8	13.5	9.4	1.7	4.8	3.4
10-15	0.25	0.31	0.33	2.6	12.0	12.2	0.9	4.2	4.4
15-20	0.29	0.42	0.35	2.1	11.9	6.5	0.7	4.2	2.3

The comparison between ψ_{soil} determined before and after the experiment from the average θ in the pot and from the intercepts of the rising and falling E phases (Fig. 6) for each soil is shown in Table 3. For the UCL, the ψ_{soil} determined from the intercept is a factor of seven greater than ψ_{soil} determined from the average θ in the pot, before the experiment, and nearly a factor of ten after the experiment. These striking differences may have been caused by the roots concentrating at the top of the pot, resulting in the soil at the base of the pot remaining relatively wet. This explanation seems plausible given the high root length density measured in the top 0 to 5 cm of the pot, compared to the lower depth increments shown in Table 2 for the UCL.

For the RCL, the substantial difference between the two estimates of ψ_{soil} determined after the experiment may have arisen from an uneven distribution of roots, and thence water, with depth in the soil (Table 3). For Table 2 shows that for the RCL, the root length density for the top 0 to 5 cm was a factor two greater than the other three depth increments, where the root length density was relatively uniform. For the repacked sand, the difference between the value of ψ_{soil} determined from the average θ in the pot, and that determined from the intercepts, is no greater than 10 kPa for measurements both before and after the experiment (Table 3).

Table 3 Comparison of ψ_{soil} determined from the average θ in the pot with ψ_{soil} determined from respective intercept on Fig. 6, before and after the experiment for the undisturbed clay-loam (UCL), repacked clay-loam soil (RCL) and repacked sand (RS).

UCL	ψ_{soil} from average θ in pot [kPa]	ψ_{soil} from intercept on Fig. 6(a) [kPa]
Before	102	760
After	113	1045
RCL	ψ_{soil} from average θ in pot [kPa]	ψ_{soil} from intercept on Fig. 6(b) [kPa]
Before	222	288
After	279	533
RS	ψ_{soil} from average θ in pot [kPa]	ψ_{soil} from intercept on Fig. 6(c) [kPa]

Before	17	7
After	23	14

Table 4 shows a summary of the key parameters used in the radial flow model for each soil.

Table 4 Summary of the key parameters used in the radial flow model for each soil. R_{plant} was derived from each particular experiment shown in Fig. 6 and D was as measured in Fig. 3. For the UCL, the experiment was modelled with the roots confined to the top third of the total soil volume (see text) and L_v as measured. For the RCL and RS, the radial flow model was run for each experiment with a range of values of L_v and the optimal fit was determined by trial and error.

Soil	L_v [cm cm^{-3}] (% of measured length)	D [m^2 s^{-1}]	R_{plant} rising E phase [kPa s μg^{-1}]	R_{plant} falling E phase [kPa s μg^{-1}]
UCL	28.7 (100)	$10x10^{-9}$	1.7	1.7
RCL	0.12 (2)	$10x10^{-9}$	1.6	2.0
RS	0.33 (10)	$1x10^{-9}$	1.5	2.9

Fig. 6 shows experimental measurements and model calculations of P as a function of E for plants growing in all three soil types.

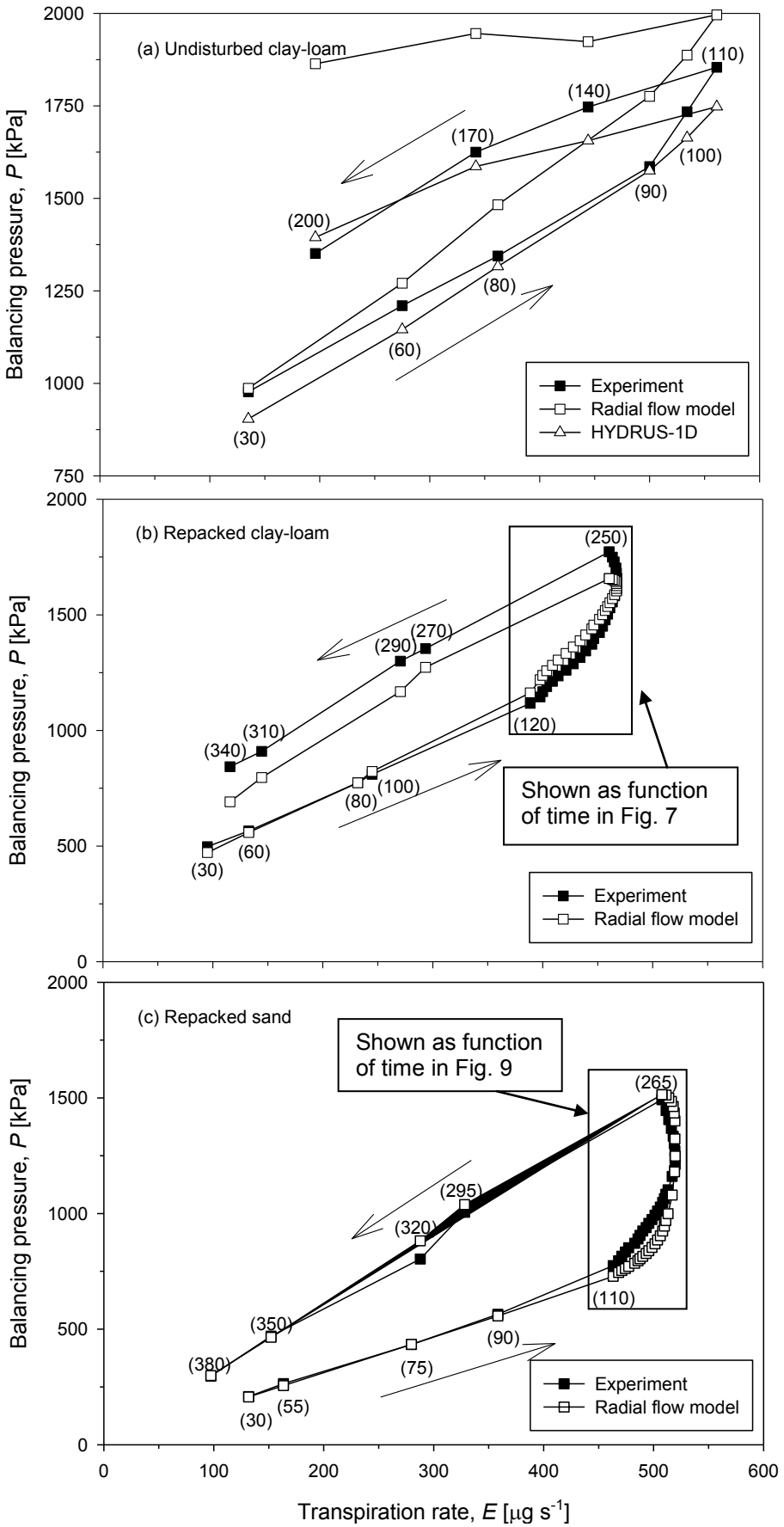

Fig. 6 For all three soil types: *P* as a function of *E*, experiment and radial flow model, and for the undisturbed clay-loam, HYDRUS-1D simulation. Input parameters for radial flow model

described in Table 4. HYDRUS-1D simulation assumed homogenous root distribution in the top 33% of the total soil volume (see text). Time [min] in parenthesis.

Fig. 7 shows experimental measurements of *P*, *E* and *g*, plotted with time for the periods shown in Fig. 6(b) and Fig. 6(c), for the repacked clay-loam and repacked sand respectively. Horizontal lines have been inserted above the plots of *E* and *g* to show the plateau and subsequent decrease in the two parameters, while at the same time, *P* continues to increase independent of *E* (note that *E* was deliberately lowered at 240 min and 265 min, for the repacked clay-loam and repacked sand respectively, as *P* was accelerating toward the limits of the apparatus).

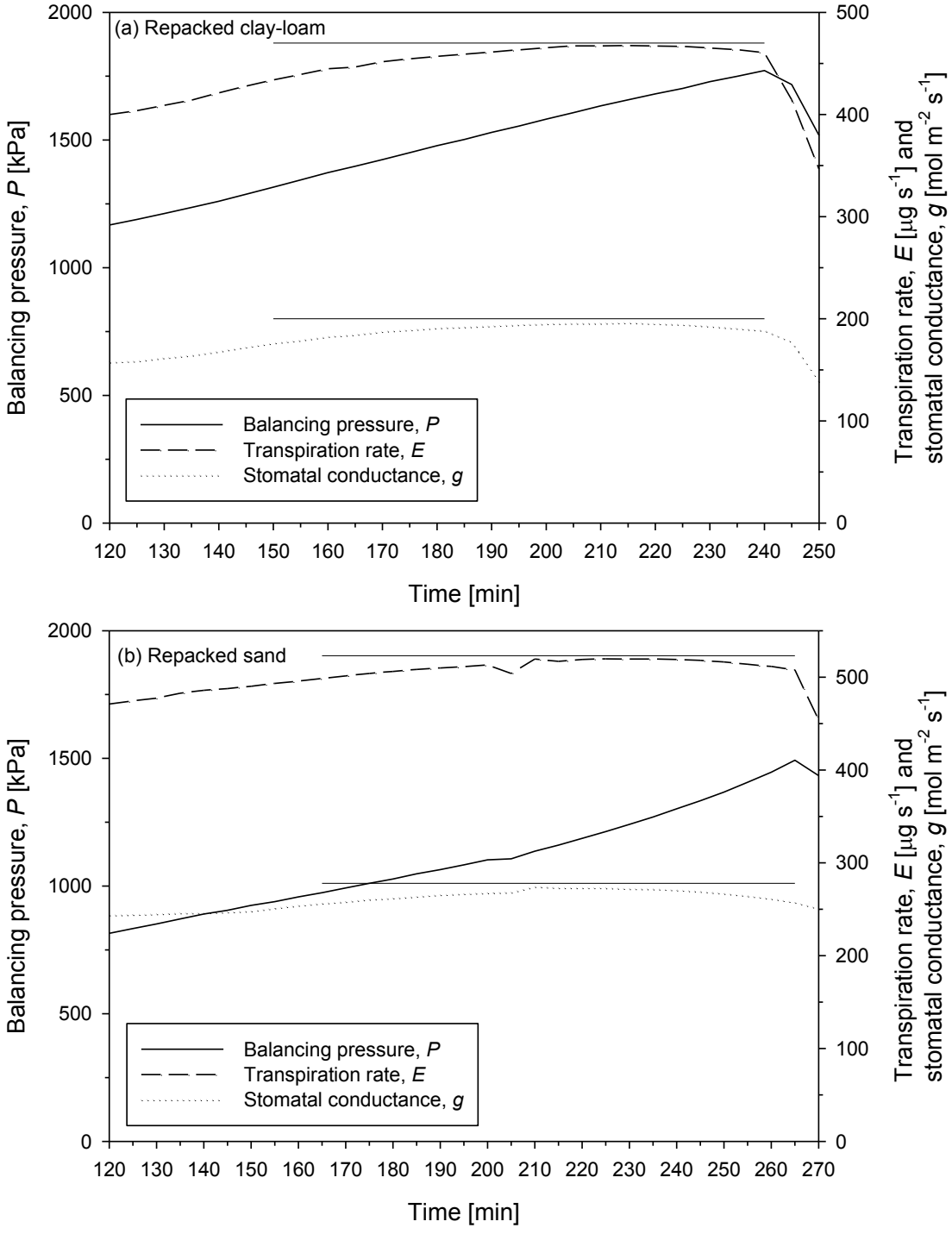

Fig. 7 Repacked clay-loam (a) and repacked sand (b): experimental measurements of *P*, *E*, and *g* plotted with time for the period shown in Fig. 6 (b) and (c) respectively. Horizontal lines above plots of *E* and *g* show the plateau and subsequent decrease in the two parameters, while *P* continues to increase independent of *E* (*E* was deliberately lowered at 240 min (a) and 265 min (b)).

Discussion

Comparison of experiment and model

Agreement between the experiment and the radial flow model was good for both the repacked clay-loam and the repacked sand (Fig. 6(b) and (c)) when the model was run using about 10% of the measured total root length density for the repacked sand, and 2% for the repacked clay-loam. These proportions of total root length are in good agreement to the 5% found by Faria et al. (2010) and, for the repacked clay-loam, close to the 1% estimated by Herkelrath et al. (1977b). However, these values are substantially less than the 30% estimated by Passioura (1980).

However, the model only matched the data during the falling phase of *E* if it was assumed that there had been a significant rise in the hydraulic resistance of the plant, or that an additional, yet constant, interfacial resistance had developed when *E* was high and *P* was rapidly increasing (discussed in further detail later). For the repacked sand, R_{plant} was increased in the model from 1.5 for the rising phase, to 2.9 kPa s μg^{-1} for the falling *E* phase. For the repacked clay-loam, R_{plant} was increased from 1.6 for the rising phase of *E* to 2.0 kPa s μg^{-1} for the falling phase.

For the undisturbed clay-loam soil, the radial flow model failed to agree with the experimental data over the entire range of the rising and falling *E* phases (Fig. 6(a)), even when the inference was made from the data in Table 2 and Table 3 that the roots were confined to the top third of the total soil volume. In contrast, the HYDRUS-1D simulation, in which water was taken up from a distributed sink throughout the top third of the total soil volume, and water flowed into that layer from wetter soil below, did agree quite well with the experiment.

Alternatively, or perhaps as well, the pots containing the undisturbed soil may have behaved as microcosms of the patterns of uptake discussed by Dardanelli et al. (2004). That is, when the copious roots at the top of the soil have taken up most of the available water there, increasing amounts of water are taken up lower in the profile, but by fewer roots. Although the soil is wetter in the lower parts of the profile, the sparseness of the roots means that the effective hydraulic resistance of the root system is substantially larger. Nevertheless, as shown by *E* continuing to increase with increasing evaporative demand, extra uptake of water at the bottom of the rooting zone by albeit sparse roots may result in *P* remaining within reasonable bounds, though rising ever faster with rising *E* when *E* is large, as shown in Fig. 6(a).

Possible interfacial resistance

Another possible explanation for the linear nature of the fall in *P* with falling *E* in the experiments with repacked clay-loam (Fig. 6(b)) and repacked sand (Fig. 6(c)), is that the roots had shrunk when *E* was high, thereby breaking some hydraulic connections between the roots and soil water which were not re-established when *E* was decreased (cf. the observations of Huck et al. (1970) who found that roots can take several hours

to recover their original diameter after high transpiration had induced root shrinkage). This could have resulted in an increased resistance to flow from the soil into the now reduced effective root length. Such behaviour would be consistent with the experience of Faiz and Weatherley (1982), who found that under high transpiration, squeezing or vibrating the soil containing sunflower roots, temporarily reduced the plant water stress. Similarly, Carminati et al. (2009) found that lupin roots shrank when the soil water content was very dry and a gap developed between the root and soil. Moreover, when the soil was irrigated again the roots swelled, but only partially refilled the gaps and some gaps remained. Postulating a constant new interfacial resistance contrasts, however, with other explorations of interfacial resistance, where the resistance was effectively a function of the soil water content (Bristow et al. 1984; Herkelrath et al. 1977b). Recently, Carminati et al. (2010 and 2011) showed that the rhizosphere may in fact have different soil hydraulic properties than the bulk soil and that these may mitigate the effects of drying soil when the transpiration rate is high.

The extra resistance invoked in Fig. 6(b) and Fig. 6(c), could be attributed in part to a build up of solutes in the rhizosphere not being accounted for in the model. The sandy soil used in this experiment may have exacerbated the possible build up of solutes in the rhizosphere (Stirzaker and Passioura 1996). However Stirzaker and Passioura (1996) watered their plants with a nutrient solution of 70 kPa osmotic pressure compared to 26 kPa in this study, so any build up of solute was less likely to occur here or would be much smaller, and the relaxation of such a build-up is unlikely to be linear with time.

The negligible drying of the bulk soil for the repacked sand (Table 3), evident in both the experimental and modelled data in Fig. 6(c), was similar to the field experiment of Carbon (1973), where the bulk soil did not dry more than 100 kPa in any of his treatments. Carbon (1973) found that the leaf water potential of sorghum plants grown on coarse sandy soil changed rapidly from no plant water stress at dawn to large negative potentials in the mid-afternoon. He concluded that despite the negligible drying of the bulk soil, the large negative leaf water potentials were due to the inability of the soil hydraulic properties to meet the potential demand of the plant.

Stomatal closure when transpiration rate is high

At the highest evaporative demand for the repacked clay-loam (Fig. 7(a)) and the repacked sand (Fig. 7(b)) E started to decrease while P was still increasing, presumably because the stomata were closing, as shown in both these figures. This is consistent with the work of Gollan et al. (1986), who used the same experimental technique in which the leaves were maintained highly turgid, and who found that wheat plants growing in drying soil closed their stomata as the soil dried and concluded that the roots were sensing the drying soil and sending signals to the shoot.

Possible role of aquaporins

Given the evidence that root signals may have been generated in the drying soil resulting in the closing of stomata noted above, such signals could be influencing the activity of aquaporins when the resistance to flow within the system is increasing (Fig. 7(a) and Fig. 7(b)). It is notable, though, that in experiments with barley growing in well-watered sand in which the water potential of the growth medium was lowered not by drying but by salinity, there was no evidence at all that R_{plant} was affected (Munns and Passioura 1984). Nevertheless, the rapid rise in P at high E coupled with

the steeper slope of P as function of E in Fig. 6(b) and Fig. 6(c), could indicate decreasing aquaporin activity, especially given that the fall in P with E was approximately linear.

Implication of findings for uptake of water from subsoils in the field

One of the aims of this paper was to see if a drawdown of water potential in the rhizosphere could substantially affect the uptake of water by roots and thence the water relations of the shoot, thereby leading to the commonly observed incomplete extraction of subsoil water by crops. Although there was some evidence of significant drawdown in the repacked soils, in which the roots were fairly evenly distributed, other influences were evidently at work, including the possible shrinkage of roots compromising their hydraulic connection with the soil, and the possible, but in our experiments, unmeasurable, effects of putative changes in the activity of aquaporins.

In the undisturbed soil, however, the radial flow model was completely unable to match the experimental data. Given the large diffusivity of water in this soil (ten times larger than expected), it is perhaps not surprising that clear evidence of a drawdown of water potential in the rhizosphere was lacking. Even when we tried to account for the evident restriction of the roots to the upper part of the pot, the radial flow model's output was nowhere near the actual data, mainly because, by confining the loss of water to only a small proportion of the pot, the radial flow model produced unrealistically low water contents and soil water potentials there. In contrast, the HYDRUS-1D simulation where the uptake of water is via a distributed sink in the top third of the pot, was in much closer agreement with the experiment and showed the possible importance of the upward flow of water within the pot (Fig. 6(a)).

A more plausible scenario of what was happening was that the plants and pots were exhibiting similar behaviour to the patterns of uptake by roots in field soils that Dardanelli et al. (2004) explored, namely that, as the topsoil dried, peak uptake of water penetrated further into the soil, where sparse roots were called upon to take up water rapidly per unit length. In effect the distributions of roots and water content with depth in the soil interacted to produce quite different behaviour from that of uniformly distributed roots in soil of uniform water content.

This scenario still, however, leaves us with the conundrum that with large values of soil water diffusivity and seemingly adequate root densities (> 0.1 cm cm^{-3}) with several weeks to extract water from the subsoil, substantial amounts of seemingly available water remained in the soil at harvest in the experiments of Kirkegaard et al. (2007), from whose site, the undisturbed subsoil was collected. Perhaps limitations to water uptake reside more within the roots themselves than within the soil.

Acknowledgements

DD received a PhD scholarship from the Cooperative Research Centre for Irrigation Futures and a PhD top-up from the CSIRO Water for Healthy Country flagship. This manuscript was written while DD received a writing up award from Charles Sturt University. We thank Michelle Watt for assistance with measuring the length and diameter of the roots and Steve Milroy for supplying the repacked sand used in this study.

References

Angus JF, Herwaarden AFV (2001) Increasing Water Use and Water Use Efficiency in Dryland Wheat. Agronomy Journal 93 (2):290-298

Bristow KL, Campbell GS, Calissendorff C (1984) The effects of texture on the resistance to water movement within the rhizosphere. Soil Sci Soc Am J 48:266-270

Campbell GS (1985) Soil physics with BASIC: transport models for soil-plant systems. Developments in soil science, vol 14. Elsevier, Amsterdam

Carbon BA (1973) Diurnal Water Stress in Plants Grown on a Coarse Soil. Australian Journal of Soil Research 11 (1):33-42

Carminati A, Moradi A, Vetterlein D, Vontobel P, Lehmann E, Weller U, Vogel H-Jr, Oswald S (2010) Dynamics of soil water content in the rhizosphere. Plant Soil 332 (1):163-176

Carminati A, Schneider CL, Moradi AB, Zarebanadkouki M, Vetterlein D, Vogel HJ, Hildebrandt A, Weller U, Schuler L, Oswald SE (2011) How the Rhizosphere May Favor Water Availability to Roots. Vadose Zone Journal 10 (3):988-998

Carminati A, Vetterlein D, Weller U, Vogel H-J, Oswald SE (2009) When Roots Lose Contact. Vadose Zone Journal: Vadose Zone Journal 8 (3):805-809

Cowan IR (1965) Transport of water in the soil-plant-atmosphere system. Journal of Applied Ecology 2:221-239

Dardanelli JL, Ritchie JT, Calmon M, Andriani JM, Collino DJ (2004) An empirical model for root water uptake. Field Crop Res 87 (1):59-71

Deery DM (2008) Water uptake by a single plant: Analysis using experimentation and modelling. PhD Thesis, Charles Sturt University, Wagga Wagga, NSW

Faiz SMA, Weatherley PE (1982) Root Contraction in Transpiring Plants. New Phytol 92 (3):333-343

Faria LN, Da Rocha MG, Van Lier QD, Casaroli D (2010) A split-pot experiment with sorghum to test a root water uptake partitioning model. Plant Soil 331 (1-2):299-311

French RJ, Schultz JE (1984) Water-Use Efficiency of Wheat in a Mediterranean-Type Environment. II. Some Limitations to Efficiency. Australian Journal of Agricultural Research 35 (6):765-775

Gardner WR (1960) Dynamic aspects of water availability to plants. Soil Science 89 (2):63-73

Gollan T, Passioura JB, Munns R (1986) Soil-Water Status Affects the Stomatal Conductance of Fully Turgid Wheat and Sunflower Leaves. Aust J Plant Physiol 13 (4):459-464

Herkelrath WN, Miller EE, Gardner WR (1977a) Water Uptake by Plants: I. Divided Root Experiments. Soil Sci Soc Am J 41:1033-1038

Herkelrath WN, Miller EE, Gardner WR (1977b) Water Uptake by Plants: II. The Root Contact Model. Soil Sci Soc Am J 41:1039-1043

Hoagland DR, Arnon DI (1950) The water culture method for growing plants without soil. California Agricultural Experiment Station Circular 347:1-32

Huck MG, Klepper B, Taylor HM (1970) Diurnal Variations in Root Diameter. Plant Physiology 45:529-530

Isbell RF (2002) The Australian soil classification, vol 4. Australian soil and land survey handbook series. CSIRO Publishing, Melbourne

Kirkegaard JA, Lilley JM, Howe GN, Graham JM (2007) Impact of subsoil water use on wheat yield. Australian Journal of Agricultural Research 58 (4):303-315

Lang ARG, Gardner WR (1970) Limitation to water flux from soils to plants. Agronomy Journal 62:693-695
Munns R, Passioura JB (1984) Hydraulic Resistance of Plants. III. Effects of Nacl in Barley and Lupin. Aust J Plant Physiol 11 (5)
Passioura JB (1980) The Transport of Water From Soil to Shoot in Wheat Seedlings. J Exp Bot 31 (120):333-345
Passioura JB (1991) Soil Structure and Plant-Growth. Australian Journal of Soil Research 29 (6):717-728
Passioura JB, Cowan IR (1968) On solving the non-linear diffusion equation for the radial flow of water to roots. Agricultural Meteorology 5 (2):129-134
Passioura JB, Munns R (1984) Hydraulic Resistance of Plants. II. Effects of Rooting Medium, and Time of Day, in Barley and Lupin. Aust J Plant Physiol 11 (5):341-350
Philip JR The physical principles of soil water movement during the irrigation cycle. In: Third Congress of International Commission on Irrigation and Drainage Proceedings, San Francisco, 1957. pp 125 - 154
Sadras VO, Angus JF (2006) Benchmarking water-use efficiency of rainfed wheat in dry environments. Australian Journal of Agricultural Research 57 (8):847-856
Simunek J, van Genuchten MT, Sejna M (2008) Development and applications of the HYDRUS and STANMOD software packages and related codes. Vadose Zone Journal 7 (2):587-600
Stirzaker RJ, Passioura JB (1996) The water relations of the root-soil interface. Plant Cell Environ 19 (2):201-208
Termaat A, Passioura JB, Munns R (1985) Shoot Turgor Does Not Limit Shoot Growth of Nacl-Affected Wheat and Barley. Plant Physiology 77 (4)
van Genuchten MT (1980) A closed-form equation for predicting the hydraulic conductivity of unsaturated soils. Soil Sci Soc Am J 44:892-898
van Lier QdJ, Metselaar K, van Dam JC (2006) Root Water Extraction and Limiting Soil Hydraulic Conditions Estimated by Numerical Simulation. Vadose Zone J 5 (4):1264-1277
Watt M, Kirkegaard JA, Rebetzke GJ (2005) A wheat genotype developed for rapid leaf growth copes well with the physical and biological constraints of unploughed soil. Functional Plant Biology 32 (8):695-706
Watt M, Magee LJ, McCully ME (2008) Types, structure and potential for axial water flow in the deepest roots of field-grown cereals. New Phytol 178 (1):135-146
White RG, Kirkegaard JA (2010) The distribution and abundance of wheat roots in a dense, structured subsoil - implications for water uptake. Plant, Cell & Environment 33 (2):133-148